OPTOELECTRONICS AND ADVANCED MATERIALS – RAPID COMMUNICATIONS Vol. 4, No. 5, May 2010, p. 735 - 739

Increase the power absorbtion efficiency in superconducting waveguides

V. A. POPESCU*
Department of Physics, University "Politehnica "of Bucharest, Splaiul Independentei 313, 060042 Bucharest, Romania

We increase the power absorption efficiency for TE_0 and TM_0 modes in superconducting traveling wave photo detectors and compensate a large part of the lost power in the substrate SiO_2 layer of a waveguide with an active superconducting YBCO layer, by using an optimized supplementary YSZ layer thickness.

(Received April 02, 2010; accepted May 20, 2010)

Keywords: Multimode waveguides, Optical planar waveguide, Superconducting films, Variational method

1. Introduction

The knowledge of optical propagation characteristics of the superconducting optical waveguides is important for the project of a new class of ultra sensitive, ultra fast and ultra slow noise detectors based on a distributed photo detection scheme of traveling wave devices [1]. The key phenomenon for the detection of light for frequencies above the gap frequency of superconductors is to annihilate Cooper pairs and create two times as many normal electrons as the broken Cooper pairs [1].

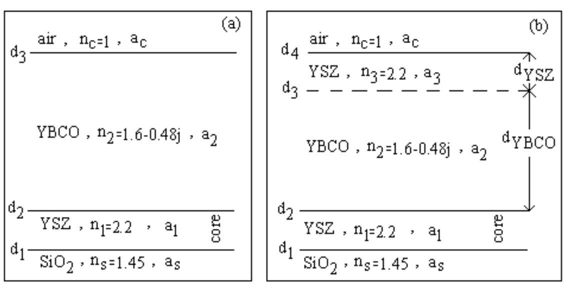

Fig. 1. (a) Schematic of a conventional superconductor planar waveguide, $d_1 = 0\mu m$, $d_2 = d_{YSZcore} = 0.04\mu m$, $d_3 = 0.24\mu m$, $d_{YBCO} = 0.2\mu m$; (b) schematic of a superconductor planar waveguide with a supplementary YSZ layer, $d_1 = 0\mu m$, $d_2 = d_{YSZcore} = 0.04\mu m$, $d_{YBCO} + d_{YSZ} = 0.2\mu m$.

The analyzed single mode waveguide [2] (Fig.1a) consists of a lossy superconductor (YBCO) layer placed on a dielectric [yttria stabilized zirconia (YSZ)] surface and this structure is enclosed by air above and a semi-infinite dielectric (SiO_2) layer below. Because YSZ dielectric core layer between the SiO_2 substrate and superconducting layer is very thin, modes TE_0 and TM_0 are not tightly confined but extend quite far from the core layer of the waveguide.

Thus, a large portion of optical power is absorbed by the YBCO layer and contributes to the photo detection process and unfortunately another great portion of power is absorbed by the substrate layer which does not contribute to the light detection.

In this paper, we introduce an improved structure (Fig.1b) which includes an optimized supplementary YSZ layer thickness sandwiched between YBCO and air layers. In this single mode structure, a larger portion of optical power, for TE_0 and TM_0 evanescent modes, is absorbed by the YBCO layer and contributes to the performance of the light detector.

2. Superconducting optical planar waveguide

The scalar-wave equation for a slab waveguide is given by

$$\frac{d^2\psi(y)}{dy^2} + k^2 n^2(y)\psi(y) = \beta^2\psi(y), \qquad (1)$$

where β is the propagation constant, k is the free space wave number, $n(y)$ is the refractive index profile

$$n(y) = \begin{cases} n_s, & for \;\; y < d_1 = 0, \\ n_i, & for \;\; d_i < y < d_{i+1}, i = 1,2, \\ n_c, & for \;\; d_3 < y, \end{cases} \qquad (2)$$

$$n(y) = \begin{cases} n_s, & for \;\; y < d_1 = 0, \\ n_i, & for \;\; d_i < y < d_{i+1}, i = 1,2,3, \\ n_c, & for \;\; d_4 < y, \end{cases} \qquad (2')$$

n_s, n_1, n_2, n_3, and n_c are the refractive index of the SiO_2 substrate, YSZ film core, YBCO film, YSZ additional film and air cladding, respectively. The effective index β/k for the TE and TM modes can be found from the dispersion equation which is obtained by applying the boundary conditions at the interfaces between different layers.

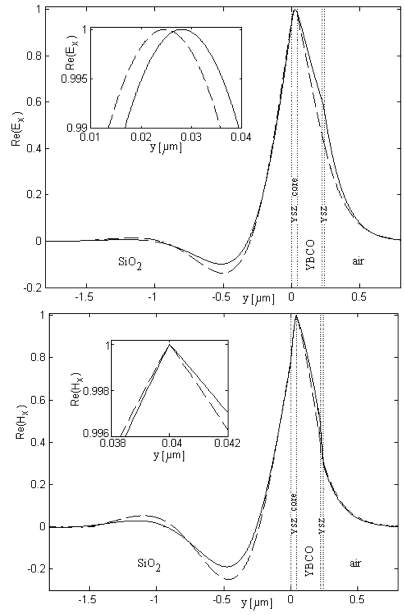

Fig. 2. The real part of the fundamental field profiles (E_x, H_x) for a waveguide (Fig.1a, - -) with d_1 = 0μm, d_2 = $d_{YSZcore}$ = 0.04μm, d_3 = 0.24μm, d_{YBCO} = 0.2μm, d_{YSZ} = 0μm, n_s = 1.45, n_1 = 2.2, n_2 = 1.6-0.48j, n_c = 1, λ = 0.85μm and for a waveguide (Fig.1b, -) with d_1 = 0μm, d_2 = $d_{YSZcore}$ = 0.04μm, d_3 = 0.22μm, d_4 = 0.24μm, d_{YBCO} = 0.18μm, d_{YSZ} = 0.02μm, n_s = 1, n_1 = 2.2, n_2 = 1.6-0.48j, n_3 =2.2, n_c = 1, λ = 0.85μm, respectively. The inset is a detail of maxima for E_x and H_x.

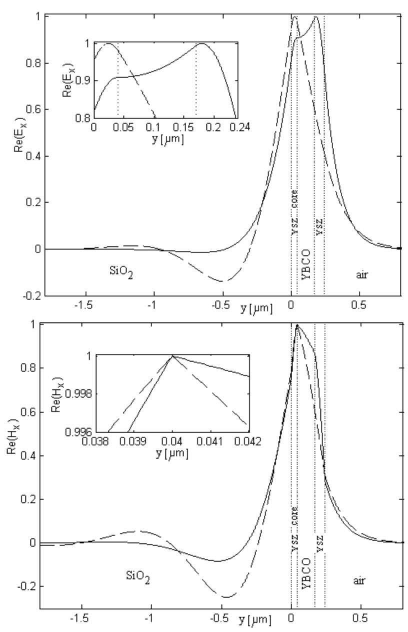

Fig. 3. The real part of the fundamental field profiles (E_x, H_x) for a waveguide (Fig.1a, - -) with d_1 = 0μm, d_2 = $d_{YSZcore}$ = 0.04μm, d_3 = 0.24μm, d_{YBCO} = 0.2μm, d_{YSZ} = 0μm, n_s = 1.45, n_1 = 2.2, n_2 = 1.6-0.48j, n_c = 1, λ = 0.85μm and for a waveguide (Fig.1b, -) with d_1 = 0μm, d_2 = $d_{YSZcore}$ = 0.04μm, d_3 = 0.17μm, d_4 = 0.24μm, d_{YBCO} = 0.13μm, d_{YSZ} = 0.07μm, n_s = 1, n_1 = 2.2, n_2 = 1.6-0.48j, n_3 =2.2, n_c = 1, λ = 0.85μm, respectively. The inset is a detail of maxima for E_x and H_x.

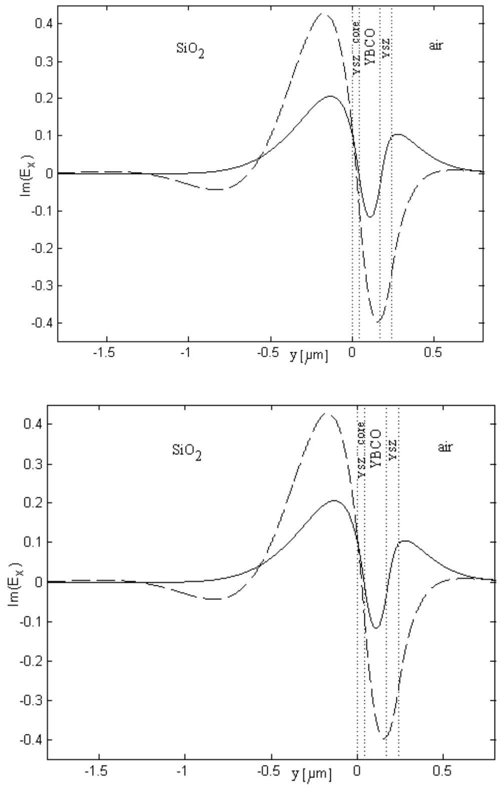

Fig. 4. The imaginary part of the fundamental field profiles (E_x, H_x) for a waveguide (Fig.1a, - -) with d_1 = 0μm, d_2 = $d_{YSZcore}$ = 0.04μm, d_3 = 0.24μm, d_{YBCO} = 0.2μm, d_{YSZ} = 0μm, n_s = 1.45, n_1 = 2.2, n_2 = 1.6-0.48j, n_c = 1, λ = 0.85μm and for a waveguide (Fig.1b, -) with d_1 = 0μm, d_2 = $d_{YSZcore}$ = 0.04μm, d_3 = 0.17μm, d_4 = 0.24μm, d_{YBCO} = 0.13μm, d_{YSZ} = 0.07μm, n_s = 1, n_1 = 2.2, n_2 = 1.6-0.48j, n_3 =2.2, n_c = 1, λ = 0.85μm, respectively. The inset is a detail of maxima for E_x and H_x.

The variational exact solution [3] of the scalar wave Eq. (1) is found from the functional

$$J_{11} = \int_{-\infty}^{d_1} [-\frac{f_s'^2}{n_s^{2\xi}} + (k n_s^{1-\xi} f_s)^2] dy \tag{3}$$

$$+\sum_{i=1}^{2} \int_{d_i}^{d_{i+1}} [-\frac{f_i'^2}{n_i^{2\xi}} + (k n_i^{1-\xi} f_i)^2] dy + \int_{d_3}^{\infty} [-\frac{f_c'^2}{n_c^{2\xi}} + (k n_c^{1-\xi} f_c)^2] dy,$$

$$J_{11} = \int_{-\infty}^{d_1} [-\frac{f_s'^2}{n_s^{2\xi}} + (k n_s^{1-\xi} f_s)^2] dy \tag{3'}$$

$$+\sum_{i=1}^{3} \int_{d_i}^{d_{i+1}} [-\frac{f_i'^2}{n_i^{2\xi}} + (k n_i^{1-\xi} f_i)^2] dy + \int_{d_4}^{\infty} [-\frac{f_c'^2}{n_c^{2\xi}} + (k n_c^{1-\xi} f_c)^2] dy,$$

subject to the constraint that

$$I_{11} = \int_{-\infty}^{d_1} \frac{f_s^2}{n_s^{2\xi}} dy + \sum_{i=1}^{2} \int_{d_i}^{d_{i+1}} \frac{f_i^2}{n_i^{2\xi}} dy + \int_{d_3}^{\infty} \frac{f_c^2}{n_c^{2\xi}} dy, \tag{4}$$

$$I_{11} = \int_{-\infty}^{d_1} \frac{f_s^2}{n_s^{2\xi}} dy + \sum_{i=1}^{3} \int_{d_i}^{d_{i+1}} \frac{f_i^2}{n_i^{2\xi}} dy + \int_{d_4}^{\infty} \frac{f_c^2}{n_c^{2\xi}} dy, \quad (4')$$

$$\beta^2 = \frac{J_{11}}{I_{11}} \quad (5)$$

where ξ reads as 0 for TE polarized waves and 1 for TM polarized waves and the exact functions f_s, f_i and f_c are given by

$$f_s(y) = A_s \exp(a_s y), \qquad y < d_1, \quad (6)$$

$$f_s(y) = A_s \exp(a_s y), \qquad y < d_1, \quad (6')$$

$$f_i(y) = A_i \cos[a_i(y - d_i)] + B_i \sin[a_i(y - d_i)], \quad d_i < y < d_{i+1}, i = 1,2 \quad (7)$$

$$f_i(y) = A_i \cos[a_i(y - d_i)] + B_i \sin[a_i(y - d_i)], \quad d_i < y < d_{i+1}, i = 1,2,3 \quad (7')$$

$$f_c(y) = A_c \exp(-a_c(y - d_3)), \quad y > d_3, \quad (8)$$

$$f_c(y) = A_c \exp(-a_c(y - d_4)), \quad y > d_4, \quad (8')$$

And

$$a_s = \sqrt{\beta^2 - (n_s k)^2}, a_c = \sqrt{\beta^2 - (n_c k)^2}, \quad a_i = \sqrt{(n_i k)^2 - \beta^2}, i = 1,2, \quad (9)$$

$$a_s = \sqrt{\beta^2 - (n_s k)^2}, a_c = \sqrt{\beta^2 - (n_c k)^2}, \quad a_i = \sqrt{(n_i k)^2 - \beta^2}, i = 1,2,3, \quad (9')$$

$$A_1 = A_s = 1, B_1 = \frac{n_1^{2\xi}}{n_s^{2\xi}} \frac{a_s}{a_1}, \quad (10)$$

$$A_1 = A_s = 1, B_1 = \frac{n_1^{2\xi}}{n_s^{2\xi}} \frac{a_s}{a_1}, \quad (10')$$

$$A_i = A_{i-1} \cos[a_{i-1}(d_i - d_{i-1})] + B_{i-1} \sin[a_{i-1}(d_i - d_{i-1})], i = 1,2, \quad (11)$$

$$A_i = A_{i-1} \cos[a_{i-1}(d_i - d_{i-1})] + B_{i-1} \sin[a_{i-1}(d_i - d_{i-1})], i = 1,2,3, \quad (11')$$

$$B_i = \frac{n_i^{2\xi}}{n_{i-1}^{2\xi}} \frac{a_{i-1}}{a_i} (B_{i-1} \cos[a_{i-1}(d_i - d_{i-1})] - A_{i-1} \sin[a_{i-1}(d_i - d_{i-1})]), i = 1,2, \quad (12)$$

$$B_i = \frac{n_i^{2\xi}}{n_{i-1}^{2\xi}} \frac{a_{i-1}}{a_i} (B_{i-1} \cos[a_{i-1}(d_i - d_{i-1})] - A_{i-1} \sin[a_{i-1}(d_i - d_{i-1})]), i = 1,2,3, \quad (12')$$

$$A_c = A_2 \cos[a_2(d_3 - d_2)] + B_2 \sin[a_2(d_3 - d_2)], \quad (13)$$

$$A_c = A_3 \cos[a_3(d_4 - d_3)] + B_3 \sin[a_3(d_4 - d_3)], \quad (13')$$

The relations (2 - 13) and (2' - 13') correspond to Fig. 1 (a) and (b), respectively.

The solutions of the dispersion equation (5) give the propagation constants *β* and the effective index *β*/*k* of the waveguide. There are numerous methods available to solve the dispersion equation [2-5].

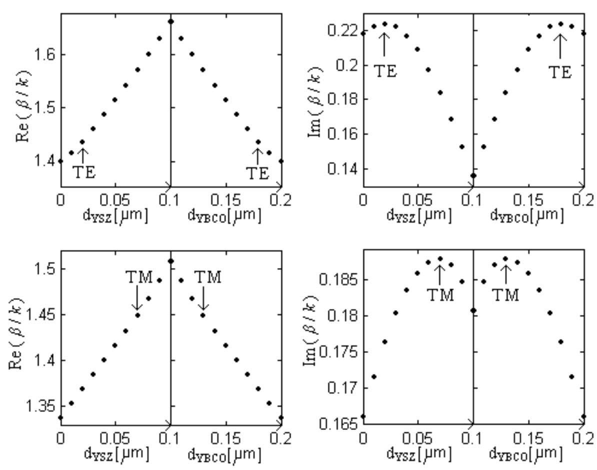

Fig. 5. Real and imaginary parts of the effective index β/k, versus a supplementary YSZ layer thickness d_{YSZ}, for TE_0 and TM_0 modes. Re (β/k) and Im (β/k) as a function of the YBCO thickness d_{YBCO}.

The total power carried by the TE (TM) mode is related to the electric (magnetic) field through the relation [6-7]:

$$P = \frac{1}{2\omega\mu_0^{1-\xi}\varepsilon_0^{\xi}} \int_{-\infty}^{\infty} \mathrm{Re}\left[\beta \frac{|\psi(y)|^2}{n^{2\xi}(y)}\right] dy, \quad (14)$$

where ξ reads as 0 for TE ($\psi = E_x$) polarized waves and 1 for TM ($\psi = H_x$) polarized waves, μ_0 is the magnetic permeability of free space, ε_0 is the permittivity in a vacuum and ω is the angular frequency. The effect of YSZ additional thickness on the confinement of the light in different parts of the waveguide structure is related to the fractional power P_i/P, where P_i is the power carried by a mode in a specific part of the waveguide.

3. Numerical results and conclusions

We have calculated the exact value of the effective index β/k for the guided modes in a waveguide (Fig.1 (a) with d_1 = 0μm, $d_2 = d_{YSZcore}$ = 0.04μm, d_3 = 0.24μm, d_{YBCO} = 0.2μm, d_{YSZ} = 0μm, n_s = 1.45, n_1 = 2.2, n_2 = 1.6-0.48j [8], n_c = 1, λ = 0.85μm, β_0/k = 1.396050-0.217941j for TE_0 and β_0/k = 1.337123-0.166104j for TM_0) and for a waveguide (Fig.1 (b) with d_1 = 0μm, $d_2 = d_{YSZcore}$ = 0.04μm, d_3 = 0.22μm, d_4 = 0.24μm, d_{YBCO} = 0.18μm, d_{YSZ} = 0.02μm, n_s = 1, n_1 = 2.2, n_2 = 1.6-0.48j, n_3 =2.2, n_c = 1, λ = 0.85μm, β_0/k = 1.434481-0.223274j for TE_0 and β_0/k = 1.368876-0.176286j for TM_0) with an additional YSZ layer but with $d_{YBCO} + d_{YSZ}$ = 0.2μm.

Fig. 2 shows the real parts of the fundamental field profiles (E_x, H_x) for these waveguides. The field amplitude has been normalized to a maximum value of unity. Also, we have calculated the exact value of the effective index β/k for a waveguide (Fig.1 (b) with d_1 = 0μm, $d_2 = d_{YSZcore}$ = 0.04μm, d_3 = 0.17μm, d_4 = 0.24μm, d_{YBCO} = 0.13μm, d_{YSZ} = 0.07μm, n_s = 1, n_1 = 2.2, n_2 = 1.6-0.48j, n_3 =2.2, n_c = 1, λ = 0.85μm, β_0/k = 1.571623-0.183812j for TE_0 and β_0/k = 1.448892-0.187739j for TM_0) with an additional YSZ layer but with $d_{YBCO} + d_{YSZ}$ = 0.2μm.

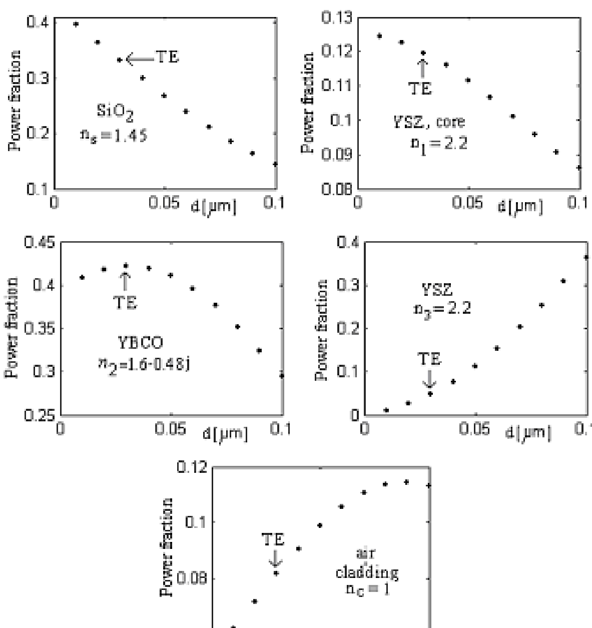

Fig. 6. Fraction of the power versus a supplementary YSZ layer thickness $d = d_{YSZ}$, carried by the fundamental mode TE_0 in different parts of the waveguide structure.

Fig. 3 shows the real parts of the fundamental field profiles (E_x, H_x) for this waveguide in comparison with the waveguide from Fig. 1 (a). Fig. 4 shows the imaginary part of the fundamental field profiles (E_x, H_x) for a waveguide (Fig. 1 (a)) with d_1 = 0μm, $d_2 = d_{YSZcore}$ = 0.04μm, d_3 = 0.24μm, d_{YBCO} = 0.2μm, d_{YSZ} = 0μm, n_s = 1.45, n_1 = 2.2, n_2 = 1.6-0.48j, n_c = 1, λ = 0.85μm and for a waveguide (Fig. 1 (b)) with d_1 = 0μm, $d_2 = d_{YSZcore}$ = 0.04μm, d_3 = 0.17μm, d_4 = 0.24μm, d_{YBCO} = 0.13μm, d_{YSZ} = 0.07μm, n_s = 1, n_1 = 2.2, n_2 = 1.6-0.48j, n_3 =2.2, n_c = 1, λ = 0.85μm, respectively.

Figs. 2 – 3 show that by increasing the thickness of the additional YSZ layer and decreasing the thickness of the active YBCO layer ($d_{YBCO} + d_{YSZ}$ = 0.2μm) the maximum of the fundamental mode E_x is shifted towards the YBCO layer, but the maximum for the fundamental mode H_x remains to a constant value y = 0.04μm.

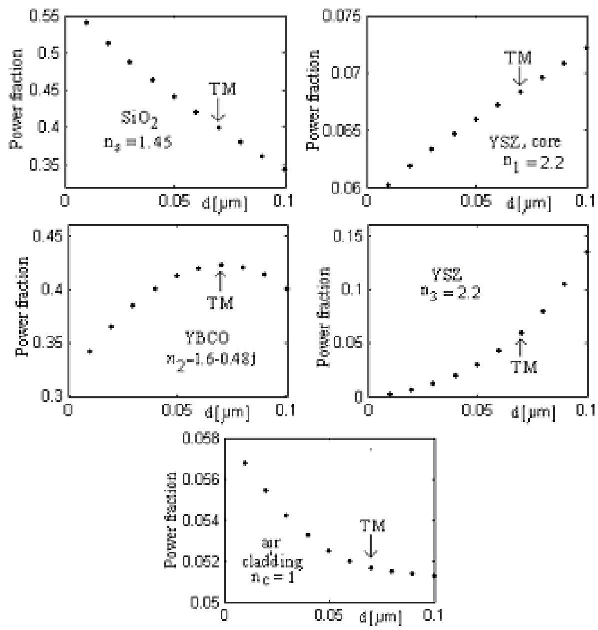

Fig. 7. Fraction of the power versus a supplementary YSZ layer thickness $d = d_{YSZ}$, carried by the fundamental mode TM_0 in different parts of the waveguide structure.

Fig. 5 shows the effect of thickening the supplementary YSZ layer on the real and imaginary parts of the effective index for TE_0 and TM_0 modes. If the thickness of the additional YSZ layer is increased, the real part of the effective index is also increased. The imaginary part of the effective index shows a maximum at small values of the additional YSZ thickness (d_{YSZ} = 0.02μm, d_{YBCO} = 0.18μm) for TE_0 mode and at high values of the additional YSZ thickness (d_{YSZ} = 0.07μm, d_{YBCO} = 0.13μm) for TM_0 mode. The maximum for the imaginary part of the effective index for TM_0 mode is smaller and shifted to higher values of the supplementary YSZ thickness in comparison with the TE_0 mode.

Figs. 6-7 show the fraction of the power, versus a supplementary YSZ layer thickness $d = d_{YSZ}$, carried by the TE_0 and TM_0 modes (per unit length in x direction) along the z axis, for different parts of the waveguide structure. With an increase in the additional YSZ layer thickness, the fraction of the power in the SiO_2 substrate is diminished and the power is increased in active YBCO layer. The fraction of the power guided in active YBCO layers shows a maximum at small values of the supplementary YSZ layer thickness ($d_{YSZ} = 0.03\mu m$, $d_{YBCO} = 0.17\mu m$) for TE_0 mode and at high values (the same as in Fig.5) of the additional YSZ layer thickness ($d_{YSZ} = 0.07\mu m$, $d_{YBCO} = 0.13\mu m$) for TM_0 mode. The maximum of the fractional power guided in superconducting layers for TM_0 mode is very close (0.42) and shifted to higher values of the additional YSZ thickness in comparison with the TE_0 mode.

Thus, although the active YBCO layer thickness was decreased, the power absorption efficiency for TE_0 and TM_0 modes in this layer is increased by using an optimized supplementary YSZ layer thickness by decreasing the lost power in the substrate SiO_2 layer of a waveguide.

Our analyses are important for engineering project of multilayer waveguides with layers consists of dielectric and superconducting materials.

References

[1] B. G. Ghamsari, A. H. Majedi, IEEE Trans. Appl. Superconduct. **17,** 590 (2007).
[2] B. G. Ghamsari, A. H. Majedi, IEEE J. Quantum Electron. **44,** 667 (2008).
[3] V. A. Popescu, J. Optoelectron. Adv. Mater. **6**, 777 (2009).
[4] L. Sun, E. Marhic, J. Opt. Soc. Amer. **B 8**, 478 (1991).
[5] K. H. Schlereth, M. Tacke, IEEE J. Quantum Electron. **26,** 626 (1990).
[6] P. Yeh, Optical Waves in Layered Media, Hoboken, NJ Wiley 2005.
[7] V. A. Popescu, N. N. Puscas, G. Perrone, J. Optoelectron. Adv. Mater.,submitted to publication.
[8] H. Kezuka, T. Masaki, N. Hosokawa, K. Hirataand, K. Ishibashi, Physica C **999**, 185 (1991).

*Corresponding author: vapopescu@yahoo.com